

Geodynamic Problems of the Junction between the Agin and Argun Zones of Transbaikalia: Evidence from U–Pb SHRIMP Dating of Rocks of the Tsugol Gabbro–Plagiogranite Massif

D. A. Lykhin^a, S. L. Presnyakov^b, G. E. Nekrasov^c, S. V. Ruzhentsev^c,
B. G. Golionko^c, and Yu. S. Balashova^c

Presented by Academician V.I. Kovalenko November 1, 2006

Received November 2, 2006

DOI: 10.1134/S1028334X07090243

The geodynamics of the junction of the Mongol–Okhotsk belt and Argun–Mamyn (Amur) continental massif is one of the key and least developed problems of Transbaikalia because of the relatively poor age constraints of magmatic complexes formed during tectonic interaction of these domains in the Precambrian and Paleozoic. Our data on the Tsugol Massif shed light on this problem.

The Tsugol gabbro–plagiogranite massif is made up of gabbro, gabbrodiorite, and diorite of the Chongul Complex and granitoids of the Zhipkhoshin Complex [1, 2]. The gabbroids and granites were ascribed to the Riphean and Carboniferous, respectively, in [2] and to the Precambrian in [1]. The massif is located at the junction of the Argun and Agin zones of Transbaikalia (Fig. 1). It extends in the meridional direction over 12 km at a maximum width of 6 km. The massif consists of several tectonic sheets plunging westward at an angle of 50°–70°. Along its eastern margin, the massif is overthrust onto the Jurassic flysch of the Argun zone, which represents the eastern part of the Argun–Mamyn microcontinent with the basement composed of Archean–Proterozoic metamorphic rocks [3]. The sedimentary cover of the microcontinent consists of Neoproterozoic–Cambrian carbonate rocks and Middle–Upper Paleozoic carbonate–terrigenous rocks. The

Mesozoic rocks comprise mainly flyschoid and volcanosedimentary series. The granitoids of the massif vary in age from the Precambrian to the Jurassic.

Along the western margin, the rocks of the Tsugol Massif plunge beneath the rocks of the Agin zone, which belongs to Mongol–Okhotsk belt considered as one of the basins of the Paleoasian ocean. The zone shows some ophiolite exposures (Prishilka belt, Sherlovaya Gora), which consist of serpentized peridotites, metagabbroids, and apobasaltic schists of the Riphean–Carboniferous age interval [1]. In terms of the paleotectonic setting, the Agin zone is considered as the Onon ensimatic island-arc system [4], which, in our opinion, is associated with the complex Devonian–Carboniferous accretion prism.

The base of the Tsugol Massif consists of unevenly layered biotite-bearing amphibole gabbro, gabbrodiorite, diorite, and subordinate amphibole–biotite plagiogranites, which form stratal bodies (5–20 m thick) conformable to gabbro layering and larger lenslike bodies (100 m thick and a few hundred meters long). This part of the massif is strongly mylonitized. The upper (relatively unaltered) part of the massif consists of amphibole diabases and gabbrodiabases with numerous equant granite bodies.

Gabbroid sample (3b-57) was taken from the lower part of the gabbro–granite massif exposed along the left tributary of the Onon River near the settlement of Tsugol (coordinates 115°35'52" E and 51°02'50" N). The gabbro sample is dark green medium-grained rock with a massive structure and typical gabbro texture. It consists of nearly equal amounts of brown green hornblende and sodic labradorite, ~5–7% of biotite, which is usually completely replaced by chlorite, and 2–3% of late quartz. Accessory minerals are apatite, zircon, and magnetite.

^a Institute of Geology of Ore Deposits, Petrography, Mineralogy, and Geochemistry, Russian Academy of Sciences, Staromonetnyi per. 35, Moscow, 119017 Russia; e-mail: liha@igem.ru

^b Karpinskii All-Russia Research Institute of Geology, Srednii pr. 74, St. Petersburg, 199026 Russia

^c Geological Institute, Russian Academy of Sciences, Pyzhevskii per. 7, Moscow, 119017 Russia

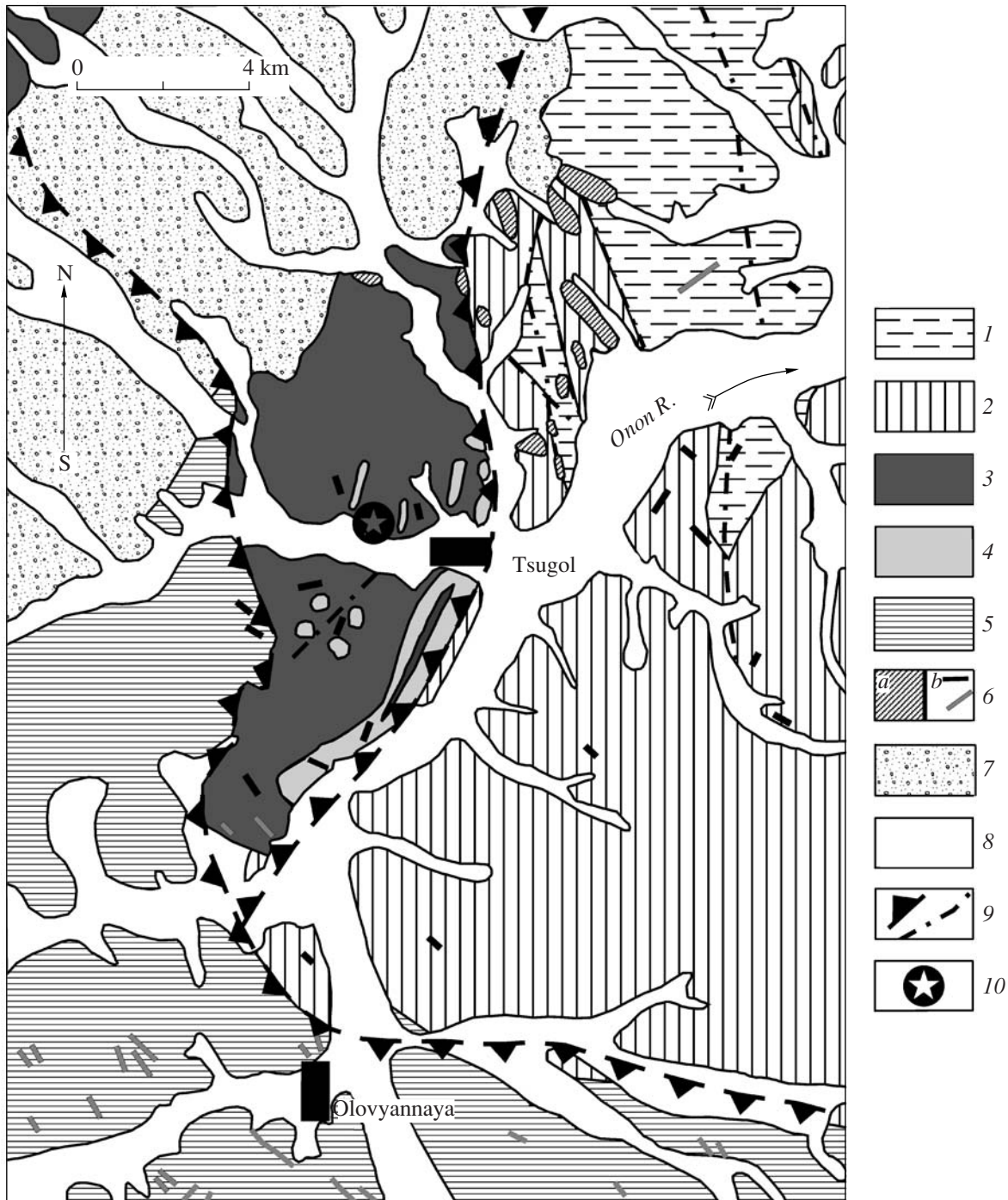


Fig. 1. Geological scheme of the area of the settlements of Tsugol and Olovyannaya. (1, 2) Argun zone: (1) Upper Devonian–Lower Carboniferous carbonate–terrigenous sequence, (2) Lower Jurassic flysch sequence; (3, 4) Tsugol Massif: (3) gabbroids of the Chongul Complex, (4) granitoids of the Zhipkhoshin Complex; (5) Agin zone: schists, quartzites, and marbles of the probably Neoproterozoic Kulinda and Onon formations; (6a) granite porphyry stocks, (6b) Late Jurassic dikes of granite porphyries and lamprophyres of the Nerchensk Complex; (7) Cretaceous–Cenozoic rocks; (8) Quaternary sediments; (9) faults and thrusts; (10) sampling locality.

The stratal amphibole–biotite plagiogranite bodies contained in the gabbroids are light gray gneissose rocks consisting of propylitized oligoclase–andesine (60–70%), quartz (30–35%), and biotite (5–7%) replaced by chlorite.

Accessory minerals are apatite, zircon, and titanite. They grade into host gabbro through gradual transition zones consisting of taxitic rocks (10–20 cm thick), which are composed of medium-grained amphibole–biotite quartz

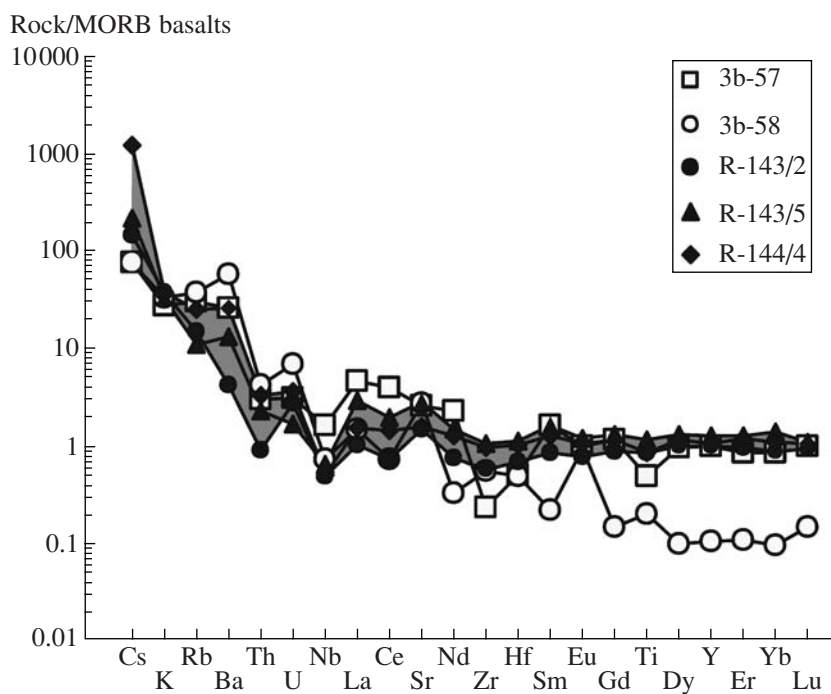


Fig. 2. MORB-normalized spidergrams. Shaded area shows the composition of the rocks of the gabbro complex.

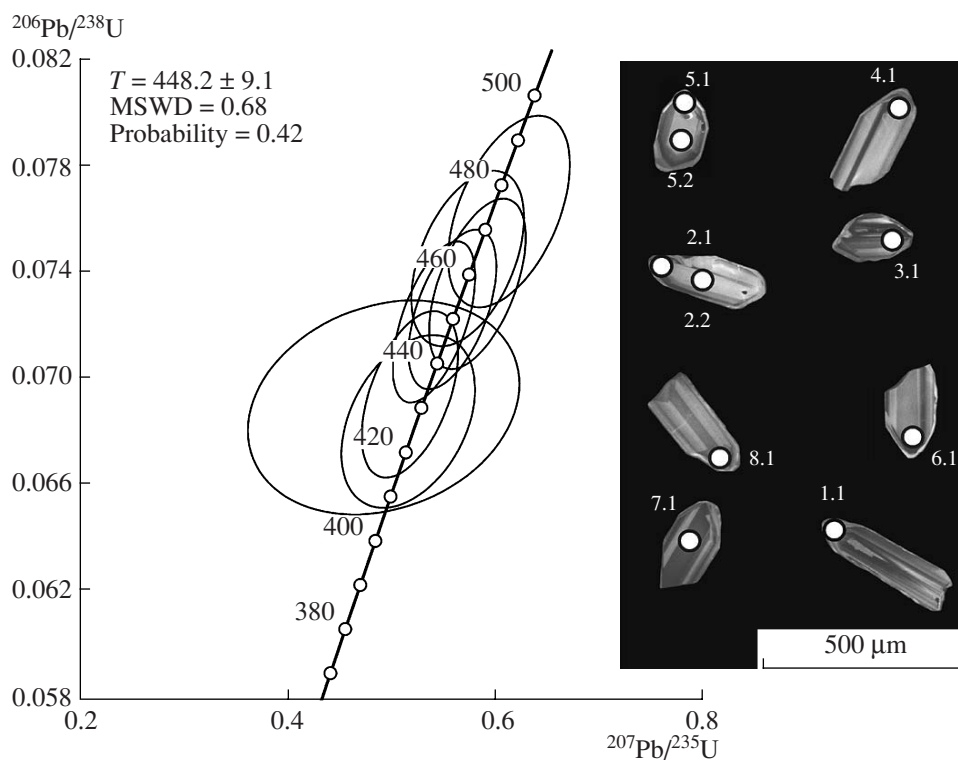


Fig. 3. U–Pb concordia diagram for zircons from the gabbro of the Chongul Complex (sample 3b-57).

Results of U–Pb isotopic studies of zircons from the gabbro of the Chongul Complex (sample 3b-57)

Sample no.	$^{206}\text{Pb}_c$, %	U, ppm	Th, ppm	$^{232}\text{Th}/^{238}\text{U}$	$^{206}\text{Pb}^*$, ppm	Age, Ma	
						$^{206}\text{Pb}/^{238}\text{U}$	
						(1)	(2)
3b-57.1.1	0.00	154	44	0.29	10.1	474.1 ± 8.8	473.2 ± 8.9
3b-57.2.1	0.02	351	123	0.36	21.7	449.4 ± 7.4	450.3 ± 7.5
3b-57.2.2	0.97	82	24	0.31	4.89	430.1 ± 9.8	432.3 ± 9.8
3b-57.3.1	0.11	239	141	0.61	15.3	463.6 ± 8	464 ± 8.2
3b-57.4.1	0.09	291	146	0.38	24.5	452.2 ± 7.3	452.4 ± 7.4
3b-57.5.1	0.00	268	78	0.30	17	457.9 ± 7.8	457.3 ± 8
3b-57.5.2	2.94	81	23	0.29	4.86	422 ± 12	434.5 ± 10
3b-57.6.1	0.00	231	100	0.45	13.8	433.1 ± 7.7	434 ± 7.8
3b-57.7.1	1.07	231	132	0.59	13.2	409.9 ± 7.7	413.4 ± 7.4
3b-57.8.1	0.35	230	72	0.32	13.6	427 ± 8	427.5 ± 8.1

Sample no.	Age, Ma		$^{238}\text{U}/^{206}\text{Pb}$	$^{207}\text{Pb}/^{206}\text{Pb}$	$^{207}\text{Pb}^*/^{235}\text{U}$ (1)	$^{206}\text{Pb}^*/^{238}\text{U}$ (1)
	$^{206}\text{Pb}/^{238}\text{U}$	$^{207}\text{Pb}/^{206}\text{Pb}$				
	(3)	(1)				
3b-57.1.1	469.4 ± 9.2	534 ± 75	13.1 ± 1.9	0.0581 ± 3.4	0.611 ± 3.9	0.0763 ± .488
3b-57.2.1	447.9 ± 7.8	378 ± 56	13.85 ± 1.7	0.0543 ± 2.5	0.539 ± 3	0.0722 ± .566
3b-57.2.2	433 ± 10	267 ± 240	14.35 ± 2.3	0.0595 ± 4.9	0.491 ± 11	0.069 ± .217
3b-57.3.1	461.9 ± 8.9	437 ± 77	13.39 ± 1.8	0.0565 ± 3	0.572 ± 3.9	0.0746 ± .463
3b-57.4.1	450.2 ± 7.8	437 ± 58	13.75 ± 1.7	0.0563 ± 2.2	0.557 ± 3.1	0.0727 ± .541
3b-57.5.1	457.5 ± 8.2	501 ± 60	13.58 ± 1.8	0.0573 ± 2.7	0.581 ± 3.3	0.0736 ± .541
3b-57.5.2	431 ± 10	–950 ± 1400	14.32 ± 2.3	0.0567 ± 5.2	0.3 ± 46	0.0677 ± .064
3b-57.6.1	431.7 ± 8.3	365 ± 72	14.39 ± 1.8	0.0539 ± 3.2	0.516 ± 3.7	0.0695 ± .499
3b-57.7.1	412.8 ± 8.1	106 ± 260	15.06 ± 1.8	0.0569 ± 3.1	0.436 ± 11	0.0657 ± .170
3b-57.8.1	426.6 ± 8.4	391 ± 110	14.55 ± 1.9	0.0573 ± 3.1	0.514 ± 5.1	0.0685 ± .377

Note: Errors are quoted at the 1 σ level; (Pb_c , Pb^*) common and radiogenic lead, respectively. Error in standard calibration was 0.72%.

- (1) Common Pb corrected to measured ^{204}Pb ;
- (2) Common Pb corrected to reliable $^{206}\text{Pb}/^{238}\text{U}$ – $^{207}\text{Pb}/^{235}\text{U}$, concordant age;
- (3) Common Pb corrected to reliable $^{206}\text{Pb}/^{238}\text{U}$ – $^{208}\text{Pb}/^{232}\text{Th}$, concordant age.

diorites and granodiorites in melanocratic bands and amphibole–biotite plagiogranites in leucocratic bands. Such relations indicate that the granite bodies are similar in age to the host gabbroids and formed via crystallization of a residual felsic melt.

Data on the chemical composition suggest that the gabbros and granites in the lower part of the massif and gabbrodiabases at the roof form low-alkali sodic series subdivided into two groups in plots of the distribution of rare and rare earth elements (Fig. 2). The first group includes rocks of the gabbro–diabase complex (R-143/2, R-143/5, R-144/4). In spidergrams, these rocks demonstrate a weakly fractionated trace-element pattern; similarity of HREE and MREE spectra to MORB basalts [5]; depletion in Nb; and enrichment in Cs, Rb, Ba, K, and La (Fig. 2). In the Th–Zr–Nb, Th–Hf–Nb, and Zr–

Nb–Y diagrams, they are plotted in the basalt field related to the destruction of continental margins [6], suggesting their formation in a suprasubduction setting of the Andean-type continental margins. The second group includes gabbro (3b-57) and granites (3b-58). The geochemical patterns of these rocks (Fig. 2) indicate that they were derived by differentiation of the parental basaltic melt corresponding in composition to the gabbro–diabase roof of the massif.

Zircons separated from gabbro are colorless (or yellow) transparent to turbid crystals. Their length varies from 122 to 353 μm . The angular fragments of long-prismatic zircons with coarse magmatic zoning and an elongation coefficient equal to 3.5–3.8 account for about 90%. The remaining 10% are represented by sub-hedral zircon grains. Inclusions are rare. The cores con-

tain 81–391 U and 23–146 $\mu\text{g/g}$ Th. The Th/U ratio is 0.29–0.61.

U–Pb zircon dating was conducted on a SHRIMP-II ion microprobe at the Center of Isotopic Research, Karpinskii All-Russia Research Institute of Geology. Hand-picked zircons were implanted in epoxy resin together with grains of TEMORA and 91500 standards. Then, the zircon grains were cut by about half of their thickness and polished. To choose analytical spots on the grain surface, we used optical (transmitted and reflected light) and cathodoluminescent images showing the internal structure and zoning of the zircons. Determination of the U–Pb ratios on SHRIMP-II was performed using the procedure described in [7]. The intensity of the primary beam of negatively charged oxygen ions was 6.5 nA, and the spot (crater) diameter was 25 μm . The data obtained were treated with the SQUID program [8]. The U–Pb ratios were normalized to that of 0.0668 in TEMORA standard zircon corresponding to an age of 416.75 Ma of this zircon [9]. Uncertainties of individual analyses (ratios and age values) are given at the 1 σ level, and errors of calculated concordant ages are quoted at the 95% confidence level. The concordia diagrams were plotted using the ISOPLOT/EX program [11].

We analyzed three spots in the cores (2.2, 5.2, and 7.1) and seven spots in the peripheral part of zircons (1.1, 1.2, 3.1, 4.1, 5.1, 6.1, and 8.1). The measurement results are summarized in the table and are shown in the U–Pb concordia diagram (table, Fig. 3). Eight of ten spots (spots 5.2 and 7.1 with high discordance were ignored) define an age of 448 ± 9.1 Ma (MSWD = 0.68), which corresponds to the Late Ordovician. Given the aforementioned relations between gabbroids and granitoids, the granitoids presumably have a similar age.

The data obtained allowed us to revise the geodynamic and structural position of the Tsugol Massif. In our opinion, rocks of this massif were formed along the

northwestern (in present-day coordinates) margin of the Argun–Mamyn (Amur) continental massif due to its destruction in the Ordovician (or Early Silurian) in the suprasubduction setting that was typical of the Andean-type margins. However, the spatiotemporal relations of the destructive processes with subduction of the oceanic lithosphere of the Mongol–Okhotsk belt remain to be solved.

ACKNOWLEDGMENTS

This work was supported by the Russian Foundation for Basic Research, project nos. 05-05-65027, 05-05-65067, and 06-05-64217.

REFERENCES

1. *Geological Map of the Chita district, Scale 1 : 500 000*, Ed. by I. G. Rutshtein (PGO Chitageologiya, Chita, 1989) [in Russian].
2. *Geological Map 1 : 200 000. Sheet M-50-VIII* (FGUGPS Chitageols"emka, Chita, 2002) [in Russian].
3. *Tectonics, Deep-Seated Structure, and Metallogeny of the Junction of the Central Asian and Pacific Belts. Explanatory Notes to Tectonic Map, Scale 1 : 1500 000* (ITG DVO RAS, Vladivostok, 2005) [in Russian].
4. Yu. A. Zorin, *Tectonophysics* **306**, 33 (1999).
5. S. Sun, A. D. McDonough, and M. J. Norry, *Geol. Soc. London Spec. Publ.* **42**, 313 (1989).
6. D. A. Wood, *Earth Planet. Sci. Lett.* **50**, 11 (1980).
7. I. S. Williams, *Rev. Econ. Geol.* **7**, 1 (1998).
8. K. R. Ludwig, *SQUID 1.00: A User's Manual* (Berkley Geochronol. Center Spec. Publ., 2000), No. 2.
9. L. P. Black, S. L. Kamo, G. M. Aleinikoff, et al., *Chem. Geol.* **200**, 155 (2003).
10. G. W. Wetherill, *Trans. Am. Geophys. Union* **37**, 320 (1956).
11. K. R. Ludwig, *Berkley Geochronol. Center Spec. Publ.*, No. 1a, 1999.